ANTIMICROBIAL AGENTS AND CHEMOTHERAPY, Mar. 1996, p. 652–658 Vol. 40, No. 3
0066-4804/96/$04.00+0
Copyright © 1996, American Society for Microbiology

Transport of the Antibacterial Agent Oxazolidin-2-One and Derivatives across Intestinal (Caco-2) and Renal (MDCK) Epithelial Cell Lines†

GIULIA RANALDI,[1] PIERFAUSTO SENECI,[2] WOLFGANG GUBA,[2] KHALID ISLAM,[2] AND YULA SAMBUY[1]*

Istituto Nazionale della Nutrizione, Rome,[1] and Lepetit Research Center, Marion Merrell Dow Research Institute, Gerenzano (Varese),[2] Italy

Received 6 June 1995/Returned for modification 20 November 1995/Accepted 22 December 1995

The transepithelial passage of the orally bioavailable antibacterial agent oxazolidin-2-one (OXa) and 10 derivatives has been studied with human intestinal (Caco-2) and canine renal (MDCK) cell lines grown on polycarbonate filters. The transepithelial passage was assayed in the apical-to-basolateral (AP-to-BL) direction and in the opposite direction (BL to AP) in both cell lines. The observed passage rates of OXa were similar in both directions in the two cell lines, suggesting passive diffusion. This was further confirmed by the fact that transport kinetics were linear as a function of initial concentration. The rates of AP-to-BL passage of OXa and seven of the derivatives in both cell lines were linearly related to lipophilicity, whether expressed as high-pressure liquid chromatography retention time or as the logarithm of the *n*-octanol–water partition coefficient (log *P*). These data suggest that the lipophilicity of OXa is important for its observed bioavailability after oral administration. Interestingly, three of the derivatives exhibited a higher passage rate than predicted by lipophilicity. Further studies indicated that this transport was saturable, similar in the two directions, and not affected by energy depletion, suggesting the presence of an additional carrier-mediated facilitated-transport mechanism.

The human intestinal cell line Caco-2 is a useful experimental model for the study of oral bioavailability of drugs, as shown in several studies by us and others (2, 20, 23, 34, 35, 46). Factors contributing to the absorption of a drug across the intestinal mucosa in vivo or across the epithelial cell monolayer in vitro include both the physicochemical characteristics of the drug and the differentiated properties of the intestinal cell (2, 4, 34, 35). Among the physicochemical characteristics that have been shown to influence the rate of transepithelial passage of drugs are lipophilicity and the capacity to form hydrogen bonds with water (7). However, a direct relationship between lipophilicity and intestinal diffusion rate appears to hold only within a narrow range of lipophilicity (45). It has also been suggested that hydrogen bonding potential, rather than lipophilicity, may be the major contributing factor in determining the intestinal or blood-brain barrier permeability of peptides (9–11, 25).

The physicochemical characteristics of the molecule determine passive passage by the paracellular or the transcellular route, while the expression of specific transport carriers by the intestinal cells allows transcellular passage by active or facilitated mechanisms. The active transport of amino acids, peptides, vitamins, and other nutrients in Caco-2 cells has been studied (1, 12–15, 17, 18, 27, 32, 33, 41–43), and, in some cases, active carriers have been shown to allow the passage of drugs by the same routes utilized by nutrients (21, 22, 35).

Oxazolidin-2-one (OXa), a synthetic antibacterial agent active against gram-positive bacteria, has been shown to be bioavailable after oral administration (39). We have studied the transport characteristics of this compound, as well as those of 10 derivatives, in epithelial intestinal Caco-2 and renal Madin-Darby canine kidney (MDCK) cell lines. Our results show that the passage of OXa occurs by passive diffusion via the transcellular route. Furthermore, examination of the passage properties of derivatives suggests that there is a good correlation between lipophilicity and transcellular passage of this class of compounds.

MATERIALS AND METHODS

Synthesis of compounds, HPLC, and spectrophotometric analysis. The synthesis, physicochemical properties, and antibacterial activities of the compounds used in this study have been described in detail previously (37). The structures and chemical formulas of the compounds used in the study are shown in Fig. 1. The compounds were analyzed by high-pressure liquid chromatography (HPLC) (Vista 5500; Varian Analytical Instruments, San Fernando, Calif.) using a LiChrosphere 100 RP-18 column (LiChro CART 125-4; E. Merck, Darmstadt, Germany). The column was developed with a linear gradient using solvent A (0.05 M ammonium formate; 90 to 30%) and solvent B (CH_3CN; 10 to 70%) for 40 min at a flow rate of 1 ml min^{-1}.

The amounts of compound passing across the cell monolayer were determined spectrophotometrically and confirmed by HPLC. The absorption maxima were determined, and the compounds were quantified by using the extinction coefficients (ε) given below (see Table 1).

Cell culture. The intestinal Caco-2 cell line (donated by A. Zweibaum, Institut National de la Santé et de la Recherche Médicale, Villejuif, France) and the renal MDCK type II cell line (donated by E. Rodriguez-Boulan, Cornell University Medical College, New York, N.Y.) were grown as previously described (34). Briefly, Caco-2 cells were routinely grown in Dulbecco modified minimal essential medium containing 25 mM glucose and 3.7 g of $NaHCO_3$ $liter^{-1}$ and supplemented with 4 mM L-glutamine, 10% heat-inactivated fetal calf serum, 1% nonessential amino acids, 100 U of penicillin ml^{-1}, and 100 μg of streptomycin ml^{-1}; the MDCK cells were grown in the same medium without addition of nonessential amino acids and with 10% donor horse serum in place of fetal calf serum. At confluency, the cells were passaged by being detached with 0.25% trypsin (1:250) and 10 mM EDTA in calcium-free and magnesium-free phosphate-buffered saline (PBS). All cell culture reagents were from Flow Laboratories International (Opera, Milan, Italy). The fluorescent dye bisbenzimide (H 33258; Boehringer Mannheim, Milan, Italy) was routinely used to screen cells for mycoplasma contamination (8).

For transport experiments, the cells were seeded on polycarbonate filter cell

* Corresponding author. Mailing address: Istituto Nazionale della Nutrizione, via Ardeatina 546, 00178 Rome, Italy. Phone: 39-6-504 2589. Fax: 39-6-503 1592.

† Paper 2380 of Special Project RAISA.

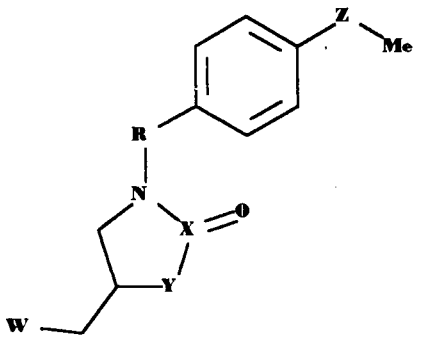

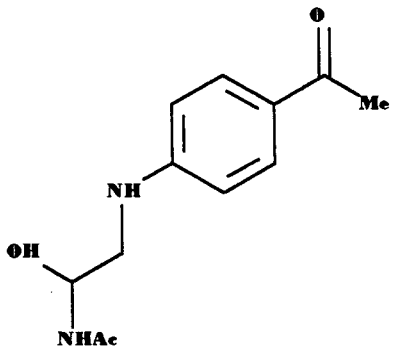

OXe

Compound	Z	R	X	Y	W
OXa	CO	absent	C	O	NHAc
OXb	CO	absent	C	O	OH
OXc	CO	absent	C	O	NH_2
OXd	CO	absent	C	O	OCOPr
OXf	CO	absent	S	NMe	NHAc
OXg	CO	absent	S	O	NHBoc
OXh	CHOH	absent	C	NH	NHAc
OXo	absent	SO_2	C	O	NHAc
OXp	CO	absent	C	O	OMs

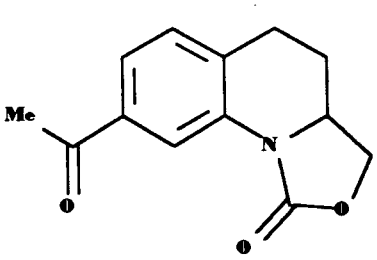

OXn

FIG. 1. Structures of OXa and derivatives tested in this study. Me, methyl; Ac, acetyl; Pr, propyl; Boc, *t*-butoxycarbonyl; Ms, methanesulfonyl.

culture chamber inserts (Transwell; 24-mm diameter, 4.7-cm^2 area, 0.45-μm pore diameter; Costar Europe, Badhoevedorp, The Netherlands) at a density of 2×10^6 cells per filter; the high seeding density allows confluency to be reached within 48 h. Caco-2 cells were allowed to differentiate at confluency for 14 to 16 days, while MDCK cells were used 6 to 8 days after seeding. The medium was regularly changed three times a week.

Transport experiments. Transport experiments were carried out as previously described (34, 35) with PBS containing 1 mM $MgCl_2$ and 1 mM $CaCl_2$ and supplemented with 5.5 mM glucose (PBS^+) as the transport buffer. The compounds were dissolved in dimethyl sulfoxide at 100 times the concentration required and were then diluted to the working concentration with PBS^+ before addition to the donor compartment; the final dimethyl sulfoxide concentration never exceeded 1% and did not affect the intactness of the cell monolayer (34). Fresh PBS^+ was added to the acceptor compartment at the start of the transport experiment. Since we were especially interested in reproducing the conditions for transmucosal transport in the luminal-to-serosal direction, the donor compartment was adjusted to pH 6.0 and the acceptor compartment was adjusted to pH 7.5 (34, 35), in analogy with the pH conditions in proximity of the brush border in the small-intestine lumen and in the submucosal compartment (46). In order to minimize the well-known effects of pH on the transport of compounds that are weak acids or bases, these pH conditions were maintained irrespective of the direction of transport across the cell monolayer (apical [AP] to basolateral [BL] or BL to AP) (34). For energy depletion, the transport buffer was supplemented with 1 mM NaN_3 and 50 mM 2-deoxyglucose in both compartments.

Prior to transport experiments, the cells were preequilibrated for 10 min in the presence of the OX compound, after which the donor and acceptor solutions were replaced. In order to avoid drug backflow, the acceptor medium was replaced after each time point with fresh prewarmed medium. The initial rates were calculated under sink conditions (2, 34, 35) from the linear portion of the compound appearance curve (i.e., before >10% of the compound had been transported). Passage rates were expressed either as nanomoles per minute per milligram, as the percentage of the initial concentration passing per hour, or as the apparent permeability coefficient (P_{app}) according to the equation P_{app} (cm s^{-1})= $\Delta Q \cdot (\Delta t \cdot 60 \cdot A \cdot C_0)^{-1}$, where $\Delta Q \cdot \Delta t^{-1}$ is the permeability rate (in micrograms per minute), C_0 is the initial concentration in the donor compartment

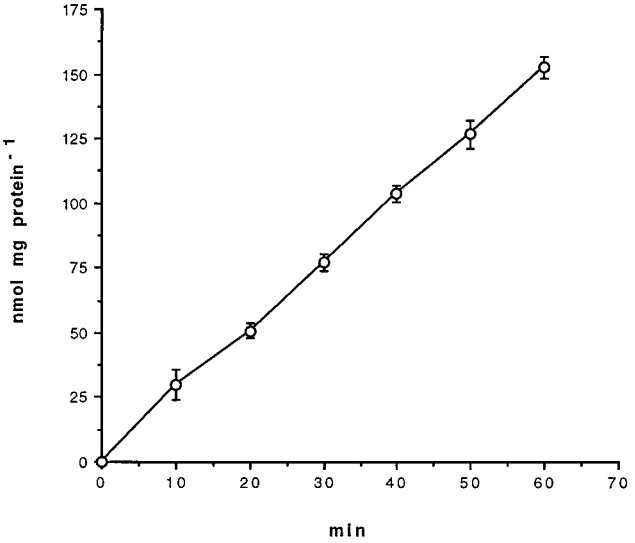

FIG. 2. Time course of the AP-to-BL passage of OXa across monolayers of Caco-2 cells. The drug was applied to the donor compartment at an initial concentration of 0.5 mM. Each point represents the mean ± standard deviation (SD) of three experiments performed in duplicate.

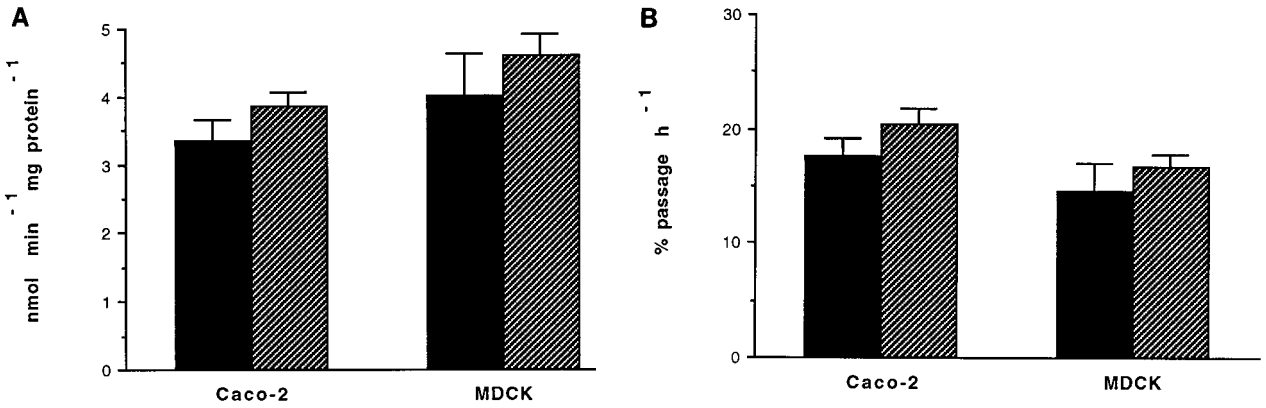

FIG. 3. Comparison of the rates of passage of OXa, expressed either as nanomoles per minute per milligram (A) or as percent passage per hour (B), in the AP-to-BL (■) and BL-to-AP (▨) directions in Caco-2 and MDCK cell monolayers. Rates of passage were calculated between 0 and 40 to 60 min from experiments similar to the one whose results are shown in Fig. 2. Data are means ± SD of three experiments performed in duplicate. The mean protein contents (± SD) of cells growing on a 4.7-cm^2 filter were 1.10 ± 0.08 mg for Caco-2 cells and 0.70 ± 0.04 mg for MDCK cells.

(in micrograms per milliliter), and A is the surface area of the membrane (in square centimeters) (2).

Before and after each experiment, the intactness of the tight junctions between the cells in filter-grown monolayers was monitored by determining transepithelial electrical resistance (TEER) and mannitol passage as previously described (35). Values for mannitol passage of intact filter-grown cell monolayers were 0.5 to 1% mannitol passage per h for both the Caco-2 and the MDCK cell lines. TEER values were 600 to 1,000 $\Omega \cdot cm^2$ for Caco-2 cells and 150 to 250 $\Omega \cdot cm^2$ for MDCK cells.

At the end of the experiment, the total protein on each filter was assayed by the method of Lowry et al. (26) after the cells were dissolved in 1 M NaOH.

Molecular modeling. Interactive modeling, energy minimization, and flexible superposition of molecules were performed with Sybyl (version 6.1a; Tripos, St. Louis, Mo.); the theoretical *n*-octanol–water partition coefficients (*P*) were calculated by Tools for Structure Activity Relationship (TSAR) (version 2.22; Oxford Molecular, Oxford, United Kingdom) for molecules for which parameters were available by using published atomic log *P* values (44).

Statistical analysis. Kinetic analysis of compound passage was performed by fitting the data by nonlinear regression analysis to theoretical equations, using the Marquardt-Levenberg algorithm (30); the computer program used for both nonlinear and linear regression analyses was Sigma Plot (Jandel Scientific, Corte Madera, Calif.).

RESULTS

The time course of passage of 0.5 mM OXa across differentiated Caco-2 cell monolayers was determined. As shown in Fig. 2, the rate of passage in the AP-to-BL direction was linear as a function of time. The rates of passage in the MDCK and Caco-2 cell monolayers and in both the AP-to-BL and BL-to-AP directions were also determined. The rates of passage in the two directions in both cell lines were similar (Fig. 3). The higher rates observed for the MDCK cell line compared with the Caco-2 cell line reflect the lower protein content of the MDCK cells per unit area (0.7 versus 1.1 mg of protein per 4.7-cm^2 filter, respectively). Indeed, the rates of passage (percent per hour) were similar for the two cell lines (Fig. 3B).

The rate of passage of OXa was further examined as a function of the initial concentration of the compound. The rate of passage was determined from the linear portion of the compound appearance curve. The passage rate increased linearly as a function of initial concentration between 0.125 and 10 mM OXa (Fig. 4), suggesting a passive diffusion mechanism. Computer fitting of the data to the equation $v = K_d \cdot [AA]$, representative of a diffusional component, where v is the velocity of passage, [AA] is the drug concentration, and K_d is the diffusion constant for a nonsaturable component, gave an apparent K_d of 5.2 ± 0.12 nmol min^{-1} mg of $protein^{-1}$ mM^{-1}.

TABLE 1. Characteristics of OXa derivatives tested in this study

Compound	Mol wt	Absorption maximum (nm)	ε (dm^3 mol^{-1} cm^{-1})
OXa	276.29	283	13,202
OXb	235.33	283	21,169
OXc	270.71	280	19,087
OXd	305.33	282	18,725
OXe	250.29	326	28,007
OXf	289.32	301	22,021
OXg	354.42	293	16,640
OXh	277.32	247	14,237
OXn	233.22	238	21,043
OXo	312.34	230	14,377
OXp	313.32	282	15,076

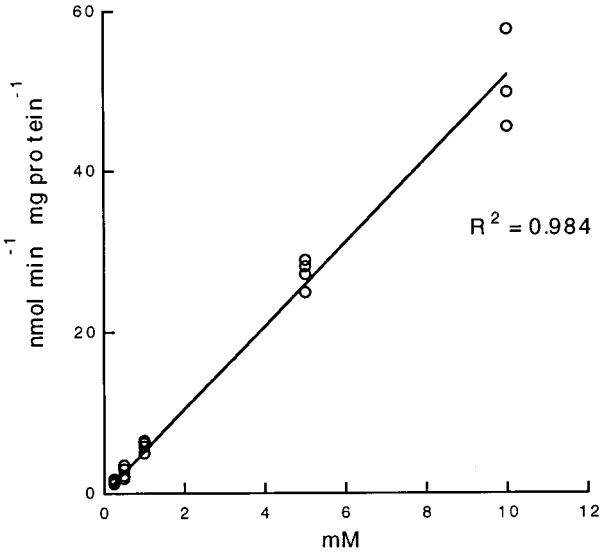

FIG. 4. Rates of AP-to-BL passage of OXa across Caco-2 cell monolayers versus initial drug concentration. Data represent linear velocities calculated from the slope of the drug appearance curve at every concentration; normally, the transport rates were calculated between 0 and 40 or 50 min (Fig. 2). Each point represents the mean of experiments performed in duplicate. Data were fitted by nonlinear regression analysis to the equation for a nonsaturable diffusion component. The apparent diffusion coefficient (K_d) calculated for this passage was 5.2 ± 0.12 nmol min^{-1} mg of $protein^{-1}$ mM^{-1}.

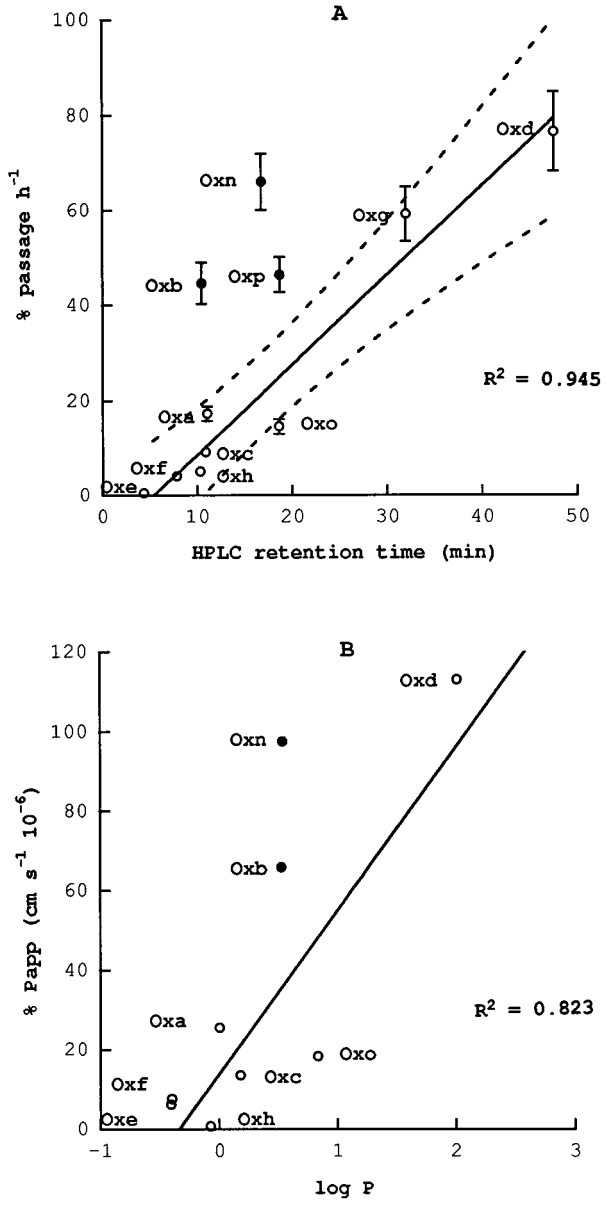

FIG. 5. Rates of AP-to-BL passage of OX compounds across Caco-2 cell monolayers versus lipophilicity. (A) Percent passage per hour versus HPLC retention time. Data are means ± SD of three to four experiments performed in duplicate. (B) Mean passage rates from panel A expressed as P_{app} and plotted versus log *P*. Linear curve fits and regression coefficients were calculated for the compounds marked with open circles, and the compounds marked with filled circles were excluded from the regression analysis. In panel A, 99% confidence intervals for the regression (dotted lines) are indicated.

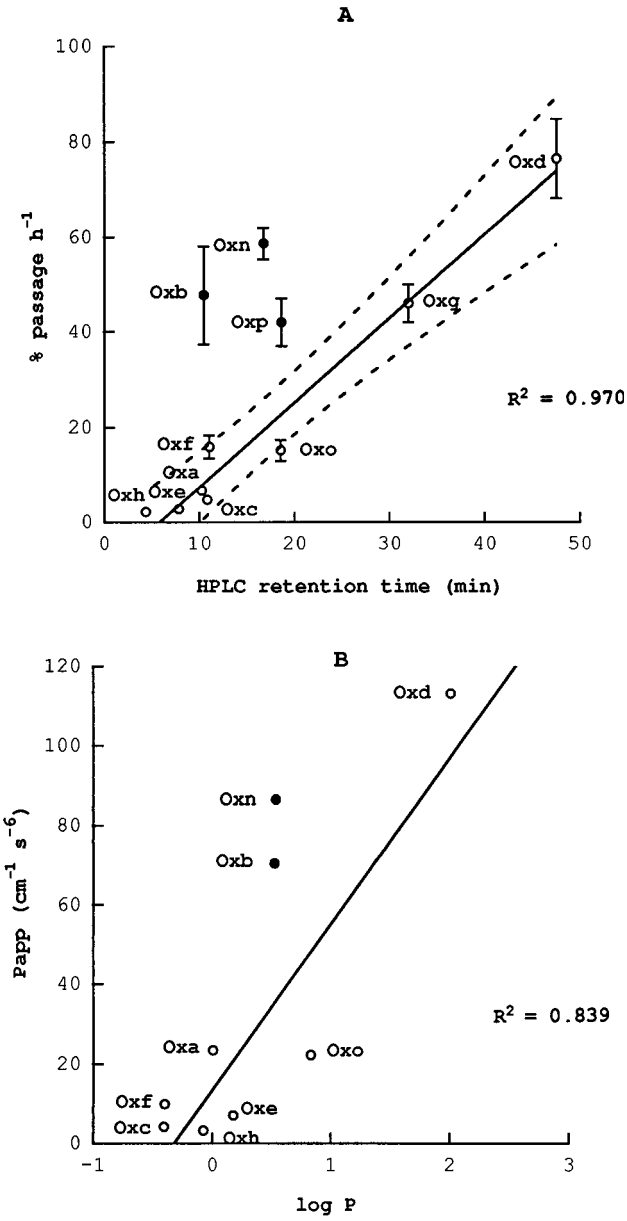

FIG. 6. Rates of AP-to-BL passage of OX compounds across MDCK cell monolayers versus lipophilicity. (A) Percent passage per hour versus HPLC retention time. Data are means ± SD of three to four experiments performed in duplicate. (B) Mean passage rates from panel A expressed as P_{app} and plotted versus log *P*. Linear curve fits and regression coefficients were calculated for the compounds marked with open circles, and the compounds marked with filled circles were excluded from the regression analysis. In panel A, 99% confidence intervals for the regression (dotted lines) are indicated.

The synthesis of several OX compounds and related heterocycles with different physical characteristics has been reported previously (37). In view of the observed passage of OXa and its behavior in the two cell lines, consistent with a passive diffusion mechanism (34), we further examined the behavior of several of these derivatives in terms of their passage across the cell monolayers. The structures, molecular weights, absorption maxima, and extinction coefficients of the derivatives used in this study are shown in Fig. 1 and Table 1).

The lipophilicity of the compounds was determined by HPLC, in which increasing retention time was indicative of increasing lipophilicity. The rates of passage of all compounds were determined at a concentration of 0.5 mM from the linear portion of the compound appearance curve. The passage rates for both Caco-2 and MDCK cells, plotted as a function of the HPLC retention times, exhibited a linear relationship for most of the compounds (Fig. 5A and 6A). A similar relationship was also observed when passage rates were expressed as P_{app} and plotted against the log of the *n*-octanol–water partition coefficient (log *P*) (Fig. 5B and 6B). However, three of the compounds tested, namely, OXb, OXn, and OXp, deviated from linearity, exhibiting a higher transport rate than would be pre-

TABLE 2. Passage of OXa and derivatives and of rifapentine across epithelial cell monolayers[a]

Compound	% Passage h^{-1} (mean ± SD)					
	Caco-2 cells			MDCK cells		
	AP to BL	BL to AP	AP to BL −E[b]	AP to BL	BL to AP	AP to BL −E
OXa	17.7 ± 1.7	20.4 ± 1.1	17.5 ± 1.8	15.9 ± 2.4	16.2 ± 1.0	15.61 ± 1.6
OXb	44.5 ± 4.3	45.0 ± 3.8	48.4 ± 4.4	47.7 ± 6.0	47.6 ± 4.8	44.12 ± 6.0
OXn	66.0 ± 5.9	66.4 ± 6.6	63.7 ± 2.8	58.6 ± 3.3	60.4 ± 5.1	55.0 ± 3.0
OXp	46.3 ± 3.7	49.7 ± 6.1	46.6 ± 1.4	42.0 ± 5.0	47.5 ± 2.3	41.3 ± 3.9
Rifapentine	31.4 ± 4.0	30.8 ± 3.0	31.9 ± 3.7	26.4 ± 3.2	28.3 ± 2.4	29.4 ± 3.3

[a] The compounds were applied to the donor compartment at 0.5 mM, and the passage is expressed as a percentage of the initial concentration from the linear portions of transport curves (see text). Data are the means ± SD of 8 to 10 determinations.
[b] −E, energy-deprived condition; passage was measured in the presence of 1 mM NaN_3 and 50 mM 2-deoxyglucose.

dicted simply on the basis of their lipophilicity. Furthermore, the behavior of these compounds was similar in the Caco-2 (Fig. 5) and MDCK (Fig. 6) cell lines, with the same three compounds exhibiting deviation from linearity.

The observed deviation from linearity of OXb, OXn, and OXp may suggest the involvement of additional transport mechanisms. The behavior of these compounds in the two cell lines, in both directions and after energy depletion, was therefore examined, using NaN_3 and 2-deoxyglucose, as previously described (35). Rifapentine was used as a control drug for passive diffusion (34), and its passage was unaffected after energy depletion. As shown in Table 2, the rates of passage in the two cell lines and in both directions of passage were similar for all compounds. Furthermore, energy depletion did not affect the rate of passage in the AP-to-BL direction.

As the passage of OXb, OXn, and OXp conforms to neither passive diffusion nor active transport, we chose to examine the transport kinetics of compound OXb in greater detail. The passage of compound OXb was therefore examined as a function of increasing initial concentration (Fig. 7). The rate of passage was linear at low concentrations but tended towards saturation at higher concentrations (4 to 10 mM). The data could be fitted by nonlinear regression analysis to the equation $v = (V_{max} \cdot [S]) \cdot (K_m + [S])^{-1}$, where v is the velocity of passage, $[S]$ is the substrate concentration, V_{max} is the maximal velocity of passage, and K_m is the substrate concentration at which the velocity is half-maximal. The apparent kinetic parameters calculated from this plot were a K_m of 9.5 ± 1.7 mM and a V_{max} of 239 ± 24 nmol min^{-1} mg^{-1}, indicating the presence of a single saturable component.

DISCUSSION

Five-membered heterocycles containing heteroatoms form a broad class of compounds, including drugs which act upon the central nervous system and gastrointestinal tract and drugs which act as cardiovascular and antitumor agents. OXa exhibits strong activity against several gram-positive bacteria and is effective in experimental infections. Furthermore, it is active in vivo after either intravenous or oral administration (39). As shown in this work, OXa can cross the epithelial cell monolayers and shows good passage across both MDCK and Caco-2 cells. We have previously shown that passage in these cell lines can be used to distinguish different mechanisms of transport (34). The similar rates of passage in the two cell lines and in the two directions are consistent with passive diffusion. Indeed, the behavior of OXa is similar to that observed with rifapentine, and the passage rate is linearly dependent on the initial concentration.

Several studies have attempted to relate the physicochemical characteristics of molecules to their passage across model cell lines, e.g., Caco-2 and MDCK. It has been shown that the passage rates of several different classes of molecules correlate with their *n*-octanol–water partition coefficients (3, 19). However, recent studies have shown that hydrogen bonding, rather than lipophilicity, is an important parameter for transport of peptides across epithelial cells (7, 10, 11, 25). In contrast to the case for peptides, the passage of OXa and derivatives suggests that lipophilicity is an important property and correlates closely to their passage across the cells. Indeed, the derivatives have various properties in terms of their electronic states, dihedral angles, and atomic distances, etc., yet regression analysis suggests a linear relationship between passage rates and lipophilicity.

Interestingly, however, a number of the OXa derivatives appear to be transported at a rate which is higher than would be predicted from their lipophilicity. Such behavior may suggest the involvement of additional transport mechanisms (e.g.,

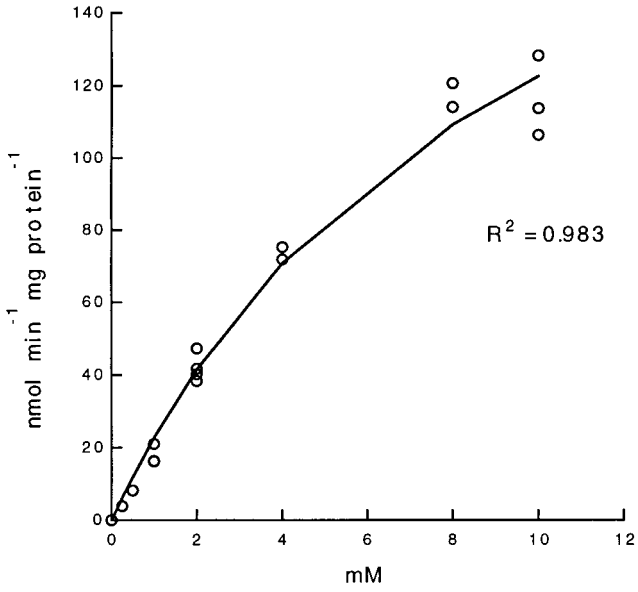

FIG. 7. Rates of AP-to-BL passage of OXb across Caco-2 cell monolayers versus initial drug concentration. Data represent linear velocities calculated from the slope of the drug appearance curve at every concentration; normally, the transport rates were calculated between 0 and 50 min. Each point is the mean of experiments performed in duplicate. Data were fitted by nonlinear regression analysis to the equation for a saturable component. The apparent kinetic parameters calculated for this transport were a K_m of 9.5 ± 1.7 mM and a V_{max} of 239 ± 24 nmol min^{-1} mg^{-1}.

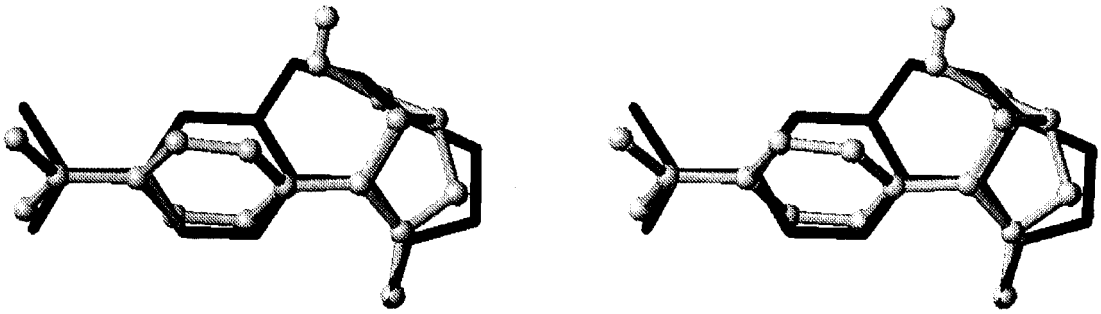

FIG. 8. Superposition of OXb (ball-and-stick representation) and OXn (black) taking into account the rotatable bonds of OXb. The centroid of the phenyl ring and the ester and carbonyl moieties of OXn were used as reference points.

active or facilitated carrier-mediated transport). We and others have previously shown that such mechanisms can be utilized by drug molecules, and active transport carriers have been identified in Caco-2 cells (21, 22, 35). In our study of D-cycloserine, we have demonstrated that use of metabolic inhibitors can drastically reduce the passage rate in Caco-2 cells (35). However, addition of metabolic inhibitors did not alter the passage rate for OXa derivatives, suggesting that an active component is not involved in their transport. In contrast to OXa, which exhibits linear kinetics of passage, OXb passage can be accounted for by a single saturable component. These results strongly argue that OXb probably uses some carrier-mediated facilitated-transport mechanism. Such mechanisms of transport have been described for different compounds (sugars and amino acids) both in the intestine in vivo (5, 6, 16, 24, 31, 40) and in vitro in the Caco-2 (28, 29, 36) and MDCK (38) cell models. The observation that OXn and OXp, like OXb, show a passage rate higher than that predicted by their lipophilicity may indicate the involvement of a similar mechanism for these derivatives. These compounds therefore differ from OXa and other derivatives whose passage rates are closely correlated with their lipophilicity. Furthermore, the observation that a similar deviation from linearity is observed in Caco-2 and MDCK cells suggests the presence of carrier-mediated facilitated transport in the two cell lines.

The higher rates of passage of OXb, OXn, and OXp can be rationalized by a common three-dimensional arrangement of structural features. As shown in Fig. 8, OXb can adopt a conformation similar to that of OXn (configured R at the aliphatic ring junction) if the centroid of the phenyl ring and the carbonyl and ester moieties are used as reference points for superimposing the compounds, with rotatable bonds taken into account. OXp can be considered a prodrug of OXb, since it was confirmed by HPLC that the methyl ester was hydrolyzed during its passage through the cells (data not shown). Summing up, the conformationally constrained OXn serves as a template for defining the relative orientation of potential hydrogen bond acceptors and the aromatic ring, common to the compounds in this study which use a facilitated-transport system.

In conclusion, we have demonstrated that the passage of OX compounds across epithelial cell monolayers is closely related to their lipophilicity. In contrast to peptides, for which hydrogen bonding appears to be an important parameter for passage (7, 25), and other drugs which exhibit a weak correlation between lipophilicity and passage (3), the OXa class of compounds represents a model drug for passive diffusion across epithelial cells. Our observations that some of the derivatives may use a facilitated carrier-mediated transport mechanism further highlight the usefulness of cell models for characterization of the mechanisms of intestinal transport.

ACKNOWLEDGMENTS

We thank Giuseppe Crocchioni (INN) for technical assistance.

This work was supported by CNR Target Project "Biotechnology and Bioinstrumentation" and by Special Project RAISA, subproject 4.

REFERENCES

1. **Alvarez-Hernandez, X., M. Smith, and J. Glass.** 1994. Regulation of iron uptake and transport by transferrin in Caco-2 cells, an intestinal cell line. Biochim. Biophys. Acta **1192:**215–222.
2. **Artursson, P.** 1990. Epithelial transport of drugs in cell culture. I. A model for studying the passive diffusion of drugs over intestinal absorptive (Caco-2) cells. J. Pharm. Sci. **79:**476–482.
3. **Artursson, P., and J. Karlsson.** 1991. Correlation between oral drug absorption in humans and apparent drug permeability coefficients in human intestinal epithelial (Caco-2) cells. Biochem. Biophys. Res. Commun. **175:**880–885.
4. **Artursson, P., and C. Magnusson.** 1990. Epithelial transport of drugs in cell culture. II. Effect of extracellular calcium concentration on the paracellular transport of drugs of different lipophilicities across monolayers of intestinal epithelial (Caco-2) cells. J. Pharm. Res. **79:**595–600.
5. **Baldwin, S. A.** 1993. Mammalian passive glucose transporters: members of an ubiquitous family of active and passive transport proteins. Biochim. Biophys. Acta **1154:**17–49.
6. **Bell, G. I., C. F. Burant, J. Takeda, and G. W. Gould.** 1993. Structure and function of mammalian facilitative sugar transporters. J. Biol. Chem. **268:** 19161–19164.
7. **Burton, P., R. Conradi, and A. Hilgers.** 1991. (B) Mechanisms of peptide and protein absorption. (2) Transcellular mechanism of peptide and protein absorption: passive aspects. Adv. Drug Deliv. Rev. **7:**365–386.
8. **Chen, T. R.** 1977. In situ detection of mycoplasma contamination in cell cultures by fluorescent Hoechst 33258 stain. Exp. Cell Res. **104:**255–262.
9. **Chikhale, E., K.-Y. Ng, P. Burton, and R. Borchardt.** 1994. Hydrogen bonding potential as a determinant of in vitro and in situ blood-brain barrier permeability of peptides. Pharm. Res. **11:**412–419.
10. **Conradi, R., A. Hilgers, N. Ho, and P. Burton.** 1992. The influence of peptide structure on transport across Caco-2 cells. II. Peptide bond modification which results in improved permeability. Pharm. Res. **9:**435–439.
11. **Conradi, R. A., A. R. Hilgers, N. F. H. Ho, and P. S. Burton.** 1991. The influence of peptide structure on transport across Caco-2 cells. Pharm. Res. **8:**1453–1460.
12. **Dix, C. J., I. F. Hassan, H. Y. Obray, R. Shah, and G. Wilson.** 1990. The transport of vitamin B12 through polarized monolayers of Caco-2 cells. Gastroenterology **98:**1272–1279.
13. **Ferruzza, S., G. Ranaldi, M. Di Girolamo, and Y. Sambuy.** 1995. Lysine transport across monolayers of human cultured intestinal cells (Caco-2): Na^+-dependent and Na^+-independent systems on different plasma membrane domains. J. Nutr. **125:**2577–2585.
14. **Fleet, J. C., A. J. Turnbull, M. Bourcier, and R. J. Wood.** 1993. Vitamin D-sensitive and quinacrine-sensitive zinc transport in human intestinal cell line Caco-2. Am. J. Physiol. **264:**G1037–G1045.
15. **Giuliano, A. R., and R. J. Wood.** 1991. Vitamin D regulated calcium transport in Caco-2 cells: unique in vitro model. Am. J. Physiol. **260:**G207–G212.
16. **Gould, G. W., and G. D. Holman.** 1993. The glucose transporter family: structure, function and tissue-specific expression. Biochem. J. **295:**329–341.
17. **Han, O., M. L. Failla, A. D. Hill, E. R. Morris, and J. C. Smith.** 1994. Inositol

phosphates inhibit uptake and transport of iron and zinc by a human intestinal cell line. J. Nutr. **124:**580–587.
18. **Hidalgo, I. J., and R. T. Borchardt.** 1990. Transport of a large neutral amino acid (phenylalanine) in a human intestinal epithelial cell line. Biochim. Biophys. Acta **1028:**25–30.
19. **Hilgers, A. R., R. A. Conradi, and P. S. Burton.** 1990. Caco-2 cell monolayers as a model for drug transport across the intestinal mucosa. Pharm. Res. **7:**902–910.
20. **Hilgers, I. J., K. M. Hillgren, G. M. Grass, and R. T. Borchardt.** 1990. Characterization of the unstirred water layer in Caco-2 cell monolayers using a novel diffusion apparatus. Pharm. Res. **7:**222–227.
21. **Hu, M., and R. Borchardt.** 1990. Mechanism of 1-α-methyldopa transport through a monolayer of polarized human intestinal epithelial cells (Caco-2). Pharm. Res. **7:**1313–1319.
22. **Inui, K., T. Okano, H. Maegawa, M. Kato, M. Takano, and R. Hori.** 1988. H^+-coupled transport of p.o. cephalosporins via dipeptide carriers in rabbit intestinal brush-border membranes: difference of transport characteristics between cefixime and cephradine. J. Pharmacol. Exp. Ther. **247:**235–241.
23. **Inui, K. I., M. Yamamoto, and H. Saito.** 1992. Transepithelial transport of oral cephalosporins by monolayers of intestinal epithelial cell line Caco-2: specific transport systems in apical and basolateral membranes. J. Pharmacol. Exp. Ther. **261:**195–201.
24. **Kilberg, M. S., B. R. Stevens, and D. A. Novak.** 1993. Recent advances in mammalian amino acid transport. Annu. Rev. Nutr. **13:**137–165.
25. **Kim, D.-C., P. S. Burton, and R. T. Borchardt.** 1993. A correlation between the permeability characteristics of a series of peptides using an in vitro cell culture model (Caco-2) and those using an in situ perfused rat ileum model for the intestinal mucosa. Pharm. Res. **10:**1710–1714.
26. **Lowry, O. H., N. J. Rosebrough, A. L. Farr, and R. J. Randall.** 1951. Protein measurement with the Folin phenol reagent. J. Biol. Chem. **193:**265–275.
27. **Ma, T. Y., D. L. Dyer, and H. M. Said.** 1994. Human intestinal cell line Caco-2: a useful model for studying cellular and molecular regulation of biotin uptake. Biochim. Biophys. Acta **1189:**81–88.
28. **Mahraoui, L., A. Rodolosse, A. Barbat, E. Dussaulx, A. Zweibaum, M. Rousset, and E. Brot-Laroche.** 1994. Presence and differential expression of SGLT1, GLUT1, GLUT 2, GLUT3 and GLUT5 hexose-transporter mRNAs in Caco-2 cell clones in relation to cell growth and glucose consumption. Biochem. J. **298:**629–633.
29. **Mahraoui, L., M. Rousset, E. Dussaulx, D. Darmoul, A. Zweibaum, and E. Brot-Laroche.** 1992. Expression and localization of GLUT5 in Caco-2 cells, human small intestine, and colon. Am. J. Physiol. **263:**G312–G318.
30. **Marquardt, D. W.** 1963. An algorithm for least squares estimation of nonlinear parameters. J. Soc. Ind. Appl. Math. **11:**431–441.
31. **Mueckler, M.** 1994. Facilitative glucose transporters. Eur. J. Biochem. **219:** 713–725.
32. **Ng, K.-Y., and R. T. Borchardt.** 1993. Biotin transport in a human intestinal epithelial cell line (Caco-2). Life Sci. **53:**1121–1127.
33. **Ramanujam, K. S., S. Seetharam, M. Ramasamy, and B. Seetharam.** 1991. Expression of cobalamin transport proteins and cobalamin transcytosis by colon adenocarcinoma cells. Am. J. Physiol. **23:**G416–G422.
34. **Ranaldi, G., K. Islam, and Y. Sambuy.** 1992. Epithelial cells in culture as a model for the intestinal transport of antimicrobial agents. Antimicrob. Agents Chemother. **36:**1374–1381.
35. **Ranaldi, G., K. Islam, and Y. Sambuy.** 1994. D-Cycloserine uses an active transport mechanism in the human intestinal cell line Caco-2. Antimicrob. Agents Chemother. **38:**1239–1245.
36. **Riley, S. A., G. Warhurst, P. T. Crowe, and L. A. Turnberg.** 1991. Active hexose transport across cultured human Caco-2 cells: characterization and influence of culture conditions. Biochim. Biophys. Acta **1066:**175–182.
37. **Seneci, P., M. Caspani, F. Ripamonti, and R. Ciabatti.** 1994. Synthesis and antimicrobial activity of oxazolidin-2-ones and related heterocycles. J. Chem. Soc. Perkin Trans. **1:**2345–2351.
38. **Sepulveda, F., and J. Pearson.** 1985. Cationic amino acid transport by two renal epithelial cell lines: LLCPK1 and MDCK cells. J. Cell. Physiol. **123:** 144–150.
39. **Slee, A., M. Wuonola, R. McRipley, I. Zajac, and A. Slee.** 1987. Oxazolidinones, a new class of synthetic antibacterial agents: in vitro and in vivo activities of DUP 105 and DUP 721. Antimicrob. Agents Chemother. **31:** 1791–1797.
40. **Thorens, B.** 1993. Facilitated gluocose transporters in epithelial cells. Annu. Rev. Physiol. **55:**591–608.
41. **Thwaites, D. T., C. D. A. Brown, B. H. Hirst, and N. L. Simmons.** 1993. Transepithelial glycylsarcosine transport in intestinal Caco-2 cells mediated by the expression of H^+-coupled carriers at both apical and basolateral membranes. J. Biol. Chem. **268:**7640–7642.
42. **Thwaites, D. T., G. T. A. McEwan, C. D. A. Brown, B. Hirst, and N. Simmons.** 1993. Na^+-independent H^+-coupled transepithelial β-alanine absorption by human intestinal Caco-2 cell monolayers. J. Biol. Chem. **268:**18438–18441.
43. **Thwaites, D. T., G. T. A. McEwan, M. J. Cook, B. Hirst, and N. Simmons.** 1993. H^+-coupled (Na^+-independent) proline transport in human intestinal (Caco-2) epithelial cell monolayers. FEBS Lett. **333:**78–82.
44. **Viswanadhan, V. N., A. K. Goshe, G. R. Revankar, and R. K. Robins.** 1994. Atomic physicalchemical parameters for the tridimensional structure-directed quantitative structure activity relationship. 4. Additional parameters for hydrophobic and dispersive interactions and their application for an automated superposition of certain naturally occurring nucleosides antibiotics. J. Chem. Inf. Comput. Sci. **29:**163–170.
45. **Wils, P., A. Warnery, V. Phung-Ba, S. Legrain, and D. Scherman.** 1994. High lipophilicity decreases drug transport across intestinal epithelial cells. J. Pharmacol. Exp. Ther. **269:**654–658.
46. **Wilson, G.** 1989. Cell culture techniques for the study of drug transport. Eur. J. Drug Metab. Pharmacokinet. **15:**159–163.